

# **Closed-loop modeling of central and intrinsic cardiac nervous system circuits underlying cardiovascular control**

Michelle M. Gee<sup>1,2</sup>, Abraham M. Lenhoff<sup>1</sup>, James S. Schwaber<sup>1,2</sup>, Babatunde A. Ogunnaike<sup>1,†</sup>, Rajanikanth Vadigepalli<sup>1,2</sup>

1 Department of Chemical and Biomolecular Engineering, University of Delaware, Newark, DE 19716

2 Daniel Baugh Institute of Functional Genomics/Computational Biology, Department of Pathology, Anatomy, and Cell Biology, Thomas Jefferson University, Philadelphia, PA 19107

## Supplemental text

### Table of Contents

1	Model equations.....	3
	Equations adapted from Park et al. 2020 .....	8
2	Model Parameters .....	26
3	Self-assessment of conformance to the Ten Simple Rules of Credible Practice in Modeling and Simulation in Healthcare.....	39
4	Sensitivity Analysis .....	58
5	Calculation of cardiovascular metric changes from Yamakawa et al. 2014 .....	61
6	Supplemental File References.....	62

## Model equations

The model, created in the SIMULINK (R2020b) platform and associated MATLAB (R2020b) code are available on GitHub (<https://github.com/Daniel-Baugh-Institute/CardiovascularControl/tree/main/v03>; ver. 3, 2022).

### Respiratory sinus arrhythmia

A gating function to modulate the outputs of the NTS that go to the NA ( $ff_{NA,input}$ ) based on the phase of the respiratory cycle was added to the extended model to capture RSA. The respiratory phase,  $s$ , varies between zero and one and resets to zero at the end of each respiratory cycle. The inspiration and post-inhalation phases of  $s$  are defined using the inhalation time ( $T_{insp}$ ) divided by the total respiratory cycle time ( $T_{resp}$ ). During inspiration, outputs from the NTS ( $ff_{NTS,output}$ ) are decreased by the gain value ( $K_{RSA}$ ), and during exhalation, outputs from the NTS are unaffected to mimic the observed NA input gating behavior.

$$ff_{NA,input} = \begin{cases} K_{RSA} * ff_{NTS,output}, & s < \frac{T_{insp}}{T_{resp}} \\ ff_{NTS,output}, & s \geq \frac{T_{insp}}{T_{resp}} \end{cases} \quad (1)$$

### Intrinsic cardiac nervous system and neuronal groups

The general equation form of neuronal groups in the ICN and brainstem

$$f_{out,j} = \frac{f_{min,j} - f_{max,j}}{1 + \left(\frac{f_{input,j}}{f_{midpt,j}}\right)^k} + f_{max,j} \quad (3)$$

This form was modified from Park (2020) to express the gain ( $k$ ) of the sigmoidal function more explicitly.<sup>1</sup> However, the functional form of the equation is the same. Parameter values for brainstem neuronal groups were modified so their behavior matched that of Park (2020) and are available in the Model parameters section. The parameters describe the maximum ( $f_{max}$ ) and minimum ( $f_{min}$ ) output firing frequency of a neuronal group, the input firing frequency to which the neuronal group is most sensitive ( $f_{midpt}$ ), and the gain ( $k$ ) describing the rate of change in output firing frequency given a change in input firing frequency.

We included in the model a first-order filter on the output of principal neurons that receive direct inputs from the dorsal motor nucleus. This filter is added to represent the slower dynamics of signal transmission due to the muscarinic receptor type that this population of neurons uses. The output, filtered ( $ff_{filtered,PN_{DMV}}$ ) is delayed by  $\tau_{PN_{DMV}}$  compared to the input ( $ff_{out,PN_{DMV}}$ ).

$$\frac{dff_{filtered,PN_{DMV}}}{dt} = \tau_{PN_{DMV}} (ff_{out,PN_{DMV}} - ff_{filtered,PN_{DMV}}) \quad (2)$$

Inputs to the local circuit neurons are a linear combination of firing frequencies from the baroreceptors ( $f_{BR}$ ), cardiopulmonary receptors ( $f_{CP}$ ), sympathetic efferent firing frequency ( $f_{esh}$ ), and vagal efferent firing frequency ( $f_{ev}$ ) multiplied by their respective gain values.

$$f_{input,LCN} = K_{LCN_{BR}}f_{br} + K_{LCN_{CP}}f_{cp} + K_{LCN_{esh}}f_{esh} + K_{LCN_{ev}}f_{ev} \quad \text{S.1}$$

### Heart period

We have modified the original model developed by Ursino (1998) and its subsequent iterations Ursino (2000), Magosso (2002), and Magosso and Ursino (2002), to account for the differences in the effect vagal activity has depending on when in the cardiac cycle it occurs.<sup>2-5</sup> The same functions as Ursino (S.2-S.5) are used to calculate the change in heart period from baseline due to vagal activity ( $\Delta T_v$ ).

$$\sigma_{T,s}(t) = \begin{cases} G_{T,s} * \ln[f_{es,h}(t - D_\theta) - f_{es,min} + 1], & f_{es,h} \geq f_{es,min} \\ 0, & f_{es,h} < f_{es,min} \end{cases} \quad \text{S.2}$$

$$\frac{d\Delta T_s}{dt}(t) = \frac{1}{\tau_{T,s}} * (-\Delta T_s(t) + \sigma_{T,s}(t)) \quad \text{S.3}$$

$$\sigma_{T,v} = G_{T,v} * f_{ev,h}(t - D_{T,v}) \quad \text{S.4}$$

$$\frac{d\Delta T_v}{dt}(t) = \frac{1}{\tau_{T,v}} * (-\Delta T_v(t) + \sigma_{T,v}(t)) \quad \text{S.5}$$

The change in heart period due to vagal activity is then modified using a gain value calculated from data on the change in heart period as a function of the timing of vagal activity in the cardiac cycle in dogs by Iano (1973) and Levy (1972).<sup>6,7</sup>

In equation S.6, the timing of the stimulus ( $t$ ) was measured as the time which had elapsed between the application of the stimulus ( $t_{fev}$ ) and the midpoint, in time ( $t_{RR,mid}$ ), of that cardiac cycle.<sup>6</sup> The gain value to be multiplied by the change in heart period was determined using Equation S.9, which is a function fit to data from Iano (1973).<sup>6</sup> The constants in equation S.9 were selected to fit the experimental data curve for the relationship between the heart period change and the timing of the stimulus relative to the midpoint of the cardiac cycle as found by Iano (1973).<sup>6</sup> Because vagal activity affects the subsequent cardiac cycle in addition to the current one, the gain values were split into  $k_{RR,t}$  and  $k_{RR,t+1}$  to modify the effect of vagal activity on heart period for the current and subsequent cardiac cycles. For example, if Iano (1973) found that heart period increased by 10 percent for vagal activity that occurred at a given point in the cardiac cycle, then the gain value would be 1.1. If the next cardiac cycle

started within a time range such that the stimulus still had an effect on it, that gain value was determined from Equation S.9 to obtain the gain value  $k_{RR,t+1}$ .

$$t = t_{RR,mid} - t_{fev} \quad \text{S.6}$$

$$k_{RR,t} = g(s)|_t \quad \text{S.7}$$

$$k_{RR,t+1} = g(s)|_{t+1} \quad \text{S.8}$$

$$g(s) = \frac{K_{RR,1}}{(\tau_{RR,1}s + 1)(\tau_{RR,2}s + 1)} - \frac{K_{RR,2}(\xi s + 1)}{(\tau_{RR,3}s + 1)(\tau_{RR,4}s + 1)} \quad \text{S.9}$$

$$T = \Delta T_s + k_{RR,t}\Delta T_v + k_{RR,t+1}\Delta T_v + T_0 \quad \text{S.10}$$

## Likelihood

A causal analysis was used to calculate the likelihood (L) that the changes in the input lung volume signal causes the changes in the output heart rate signal (y). Likelihood is calculated from the difference between the output heart rate and the predicted heart rate ( $y_{pred}$ ) calculated by Gaussian process regression.<sup>8,9</sup>

$$L = -\ln(\text{var}(y - y_{pred})) \quad (4)$$

## Equations adapted from Park et al. 2020

*We would like to emphasize that this text is from source material (Park et al. 2020) and is provided here for the readers' convenience.<sup>1</sup> Interested readers are recommended to review this paper for a detailed description of the model.*

Table S.1 Hemodynamic variables

<b>Model parameters</b>	<b>Corresponding physiological parameter</b>
$P_j$	Intravascular pressure
$V_{u,j}$	Unstressed volume
$F_j$	Blood flow
$C_j$	Compliance
$L_j$	Inertance
$R_j$	Resistances
$F_{o,r}$	Flow out of right ventricle
$F_{o,l}$	Flow out of left ventricle

### Vascular system

Conservation of mass at pulmonary arteries ( $pa$ )

$$\frac{dP_{pa}}{dt} = \frac{1}{C_{pa}} (F_{o,r} - F_{pa}) \quad \text{S.11}$$



Balance of forces at pulmonary arteries ( $\rho a$ )

$$\frac{dF_{pa}}{dt} = \frac{1}{L_{pa}} (P_{pa} - P_{pp} - R_{pa} * F_{pa}) \quad \text{S.12}$$

The inertance represents the change in pressure required to cause a change in flowrate of a fluid. Due to the large diameter of the arteries, inertances affect hemodynamic behavior more noticeably in these blood vessels than in the smaller diameter veins.

Conservation of mass at pulmonary peripheral circulation ( $\rho p$ )

$$\frac{dP_{pp}}{dt} = \frac{1}{C_{pa}} \left( F_{pa} - \frac{P_{pp} - P_{pv}}{R_{pp}} \right) \quad \text{S.13}$$

Conservation of mass at pulmonary veins ( $\rho v$ )

$$\frac{dP_{pv}}{dt} = \frac{1}{C_{pv}} \left( \frac{P_{pp} - P_{pv}}{R_{pp}} - \frac{P_{pv} - P_{la}}{R_{pv}} \right) \quad \text{S.14}$$

Conservation of mass at systemic arteries ( $sa$ )

$$\frac{dP_{sa}}{dt} = \frac{1}{C_{sa}} (F_{o,l} - F_{sa}) \quad \text{S.15}$$

Force balance at systemic arteries

$$\frac{dF_{sa}}{dt} = \frac{1}{L_{sa}} (P_{sa} - P_{sp} - R_{sa} * F_{sa}) \quad \text{S.16}$$

Conservation of mass at peripheral systemic circulation – splanchnic, extrasplanchnic, and lower body compartments (*sp*, *ep*, *mp*)

$$\frac{dP_{sp}}{dt} = \frac{1}{C_{sp} + C_{ep} + C_{mp}} * \left( F_{sa} - \frac{P_{sp} - P_{sv}}{R_{sp}} - \frac{P_{sp} - P_{ev}}{R_{ep}} - \frac{P_{sp} - P_{mv}}{R_{lb}} \right) \quad \text{S.17}$$

Where

$$\left( R_{lb} = \frac{1}{R_{mp}} + \frac{1}{R_d} \right) \quad \text{S.17.1}$$

NOTE: To incorporate the effects of varying abdominal pressure  $P_{abd}$  due to respiration, transmural pressure is calculated by subtracting  $P_{abd}$  from  $P_{sp}$ .

Equations for  $P_{abd}$  are provided in later equations.

$$P_{sp-trans} = P_{sp} - P_{abd} \quad \text{S.17.2}$$

This transmural pressure is subsequently used to determine downstream pressures.

Conservation of mass at extrasplanchnic venous circulation (*ev*)

$$\frac{dP_{ev}}{dt} = \frac{1}{C_{ev}} \left( \frac{P_{sp} - P_{ev}}{R_{ep}} - \frac{P_{ev} - P_{tv}}{R_{ev}} - \frac{dV_{u,ev}}{dt} \right) \quad \text{S.18}$$

Conservation of mass at skeletal muscle, part of the lower body (*mv*)

$$\frac{dP_{mv}}{dt} = \frac{1}{C_{mv}} \left( \frac{P_{sp} - P_{mv}}{R_{lb}} - \frac{P_{mv} - P_{tv}}{R_{mv}} - \frac{dV_{u,mv}}{dt} \right) \quad \text{S.19}$$

Conservation of mass at thoracic vein (*tv*)

$$\frac{dP_{tv}}{dt} = \frac{1}{C_{tv}} \left( \frac{P_{mv} - P_{tv}}{R_{mv}} + \frac{P_{ev} - P_{tv}}{R_{ev}} + \frac{P_{sv} - P_{tv}}{R_{ev}} - \frac{P_{tv} - P_{ra}}{R_{tv}} \right) \quad \text{S.20}$$

NOTE: To incorporate the effects of varying thoracic pressure  $P_{thor}$  due to respiration, transmural pressure is calculated by subtracting  $P_{thor}$  from  $P_{tv}$ .

Equations for  $P_{thor}$  are provided in later equations.

$$P_{tv-trans} = P_{tv} - P_{thor} \quad \text{S.20.1}$$

Conservation of mass determines splanchnic venous circulation, which assumes total blood volume ( $V_t$ ) is known.

$$\begin{aligned}
P_{sv} = \frac{1}{C_{sv}} & \left( V_t - C_{sa} * P_{sa} - (C_{sp} + C_{ep} + C_{mp}) * P_{sp} - C_{ev} \right. \\
& * P_{ev} - C_{mv} * P_{mv} - C_{tv} * P_{tv} - C_{ra} * P_{ra} \\
& - V_{ra} - C_{pa} * P_{pa} - C_{pp} * P_{pp} - C_{pv} * P_{pv} \\
& \left. - C_{la} * P_{la} - V_{lv} - V_u \right)
\end{aligned} \tag{S.21}$$

Here,  $V_{rv}$  and  $V_{lv}$  are the volumes of the right and left ventricles.  $V_u$  is the total unstressed volume, defined by:

### Pulsatile (left) heart

Conservation of mass at left atrium (la)

$$\frac{dP_{la}}{dt} = \frac{1}{C_{la}} \left( \frac{P_{pv} - P_{la}}{R_{pv}} - F_{i,l} \right) \tag{S.22}$$

$F_{i,l}$  refers to the flow into the left ventricle, determined by the following mass balance:

$$F_{i,l} = \begin{cases} 0, & P_{la} < P_{lv} \\ \frac{P_{la} - P_{lv}}{R_{la}}, & P_{la} \geq P_{lv} \end{cases} \tag{S.23}$$

Ventricular volume is calculated using the following equation:

$$\frac{dV_{lv}}{dt} = F_{i,l} - F_{o,l} \tag{S.24}$$

And flow out of the left ventricle ( $F_{o,l}$ ) is determined by:

$$F_{o,l} = \begin{cases} 0, & P_{max,lv} < P_{sa} \\ \frac{P_{max,lv} - P_{sa}}{R_{lv}}, & P_{max,lv} \geq P_{sa} \end{cases} \quad \text{S.25}$$

$P_{max,lv}$  represents the isometric pressure of the left ventricle. This value is used to determine ventricular pressure over the course of the cardiac cycle.  $R_{lv}$  represents the viscous resistance of the left ventricle and is assumed to be proportional to  $P_{max,lv}$  where:

$$R_{lv} = k_{R,lv} * P_{max,lv} \quad \text{S.26}$$

$k_{R,lv}$  is a constant parameter.

Instantaneous pressure in the left ventricle represents the difference between the isometric pressure ( $P_{max,lv}$ ) and viscous losses, therefore:

$$P_{lv} = P_{max,lv} - R_{lv} * F_{o,l} \quad \text{S.27}$$

Isometric pressure is time-dependent and varies throughout the cardiac cycle. The base model by Ursino assumes that isometric pressure/volume can be characterized by an exponential function during diastole, when the ventricle is relaxed, and by a linear function at the end of systole, when the ventricle is contracted maximally. Thus, isometric pressure transitions between an exponential and linear function over the course of the cardiac cycle.

$$P_{max,lv} = \varphi(t) * E_{max,lv} * (V_{lv} - V_{u,lv}) + [1 - \varphi(t)] * P_{0,lv} * (\exp(k_{E,lv} * V_{lv}) - 1) \quad \text{S.28}$$

Where  $0 \leq \varphi(t) \leq 1$

$E_{max,lv}$  is the ventricular elastance at the maximal contraction of the ventricle.  $V_{u,lv}$  is the corresponding unstressed volume of the ventricle and is the x-axis intercept of the end-systolic pressure/volume function.  $P_{0,lv}$  and  $k_{E,lv}$  are constant parameters that describe the monoexponential pressure/volume function at diastole.

The term  $\varphi(t)$  represents the “activation function” of the ventricle. When  $\varphi(t) = 1$ , the ventricle is at maximum contraction, when  $\varphi(t) = 0$ , it is at complete relaxation. This activation function is defined as:

$$\varphi(t) = \begin{cases} \sin^2 \left[ \frac{\pi * T(t)}{T_{sys}(t)} * u \right], & 0 \leq u \leq \frac{T_{sys}}{T} \\ 0, & \frac{T_{sys}}{T} \leq u \leq 1 \end{cases} \quad \text{S.29}$$

$T$  represents the heart period (i.e. inverse of heart rate).  $T_{sys}$  is the duration of systole and  $u$  is a dimensionless variable ranging between 0 and 1 and represents the fraction of the cardiac cycle. A value of  $u = 0$  corresponds to the beginning of systole. This variable has been modeled as an integral pulse frequency modulation function (Bailón et al. 2011).

$$u(t) = \text{frac} \left[ \int_{t_0}^t \frac{1}{T(t)} d\tau + u(t_0) \right] \quad \text{S.30}$$

The fractional part of this equation,  $\text{frac} [ ]$ , indicates that the variable  $u(t)$  is reset to zero as soon as the value reaches a value of 1.

The duration of systole is determined by the following equation:

$$T_{sys} = T_{sys,0} - k_{sys} * \frac{1}{T} \quad \text{S.31}$$

Where  $k_{sys}$  and  $T_{sys,0}$  are constant parameters. A separate set of equations similar to equations S.22-S.31 are used to describe the right heart as well.

### **Pulsatile (right) heart**

Conservation of mass at right atrium (ra)

$$\frac{dP_{ra}}{dt} = \frac{1}{C_{ra}} \left( \frac{P_{tv} - P_{ra}}{R_{tv}} - F_{i,l} \right) \quad \text{S.32}$$

Flow into right ventricle:

$$F_{i,r} = \begin{cases} 0, & P_{ra} < P_{rv} \\ \frac{P_{ra} - P_{rv}}{R_{ra}}, & P_{ra} \geq P_{rv} \end{cases} \quad \text{S.33}$$

Volume of right ventricle:

$$\frac{dV_{rv}}{dt} = F_{i,r} - F_{o,r} \quad \text{S.34}$$

Flow out of right ventricle:

$$F_{o,r} = \begin{cases} 0, & P_{max,rv} < P_{pa} \\ \frac{P_{max,rv} - P_{pa}}{R_{rv}}, & P_{max,rv} \geq P_{pa} \end{cases} \quad \text{S.35}$$

Viscous resistance of right ventricle:

$$R_{rv} = k_{R,rv} * P_{max,rv} \quad \text{S.36}$$

Instantaneous pressure in right ventricle:

$$P_{rv} = P_{max,rv} - R_{rv} * F_{o,r} \quad \text{S.37}$$

Isometric pressure in right ventricle:

$$P_{max,rv}(t) = \varphi(t) * E_{max,rv} * (V_{rv} - V_{u,rv}) + [1 - \varphi(t)] * P_{0,rv} * (\exp(k_{E,rv} * V_{rv}) - 1) \quad \text{S.38}$$

Where  $\varphi(t)$  is determined from equations S.29-S.30.



## Afferent input types

Baroreceptors are modeled using a linear derivative first-order dynamic function and a sigmoidal static characteristic function in series, described by the following equations:

$$\tau_p \frac{d\dot{P}}{dt} = P_{br} + \tau_z * \frac{dP_{br}}{dt} - \dot{P} \quad \text{S.39}$$

$$f_{br} = \left[ f_{min} + f_{max} * \exp\left(\frac{\dot{P} - P_n}{k_a}\right) \right] / \left[ 1 + \exp\left(\frac{\dot{P} - P_n}{k_a}\right) \right] \quad \text{S.30}$$

Here,  $\tau_p$  and  $\tau_z$  are time constants for the real pole and real zero in the linear dynamic block.  $P_{br}$  is the arterial pressure measured by the baroreceptors.  $\dot{P}$  is the output variable of the dynamic block (with dimensions of pressure).  $f_{br}$  is the frequency of spikes in the afferent fibers.  $f_{min}$  and  $f_{max}$  are the lower and upper saturation limits of the frequency discharge of the baroreceptors.  $P_n$  is the intrasinus pressure at the central point of the sigmoidal curve and  $k_a$  is a constant parameter (with dimensions of pressure).

Cardiopulmonary receptors are modeled using a first-order low-pass filter in series with the same sigmoidal static characteristic function type used to model the baroreceptors. Because cardiopulmonary receptors depend on transmural pressure at the pulmonary veins, this pressure difference is used as an input to first-order low-pass filter:

$$\tau_{cp} \frac{dP_l}{dt} = -P_l + (P_{pv} - P_{thor}) \quad \text{S.41}$$

$$f_{cp} = \frac{f_{max,l}}{1 + \exp\left(\frac{P_{tn} - P_l}{k_l}\right)} \quad \text{S.42}$$

Here  $P_{pv} - P_{thor}$  is the transmural pressure at the pulmonary vein or input value to the low-pass filter function.  $P_l$  is the output variable of the low-pass filter.  $f_{cp}$  is the spike frequency of the afferent fibers from the cardiopulmonary receptors and  $f_{max,l}$  is the upper saturation limit of the frequency discharge of these receptors, the lower limit being zero.  $P_{tn}$  represents the pulmonary venous pressure at the central point of the sigmoid curve.  $k_l$  is another constant that determines the slope of the sigmoid curve, or sensitivity of the cardiopulmonary receptors.

Lung stretch receptors are modeled using a first-order low-pass filter:

$$\frac{df_{lr}}{dt} = \tau_{lung} * (-f_{lr} + G_{al} * V_{lung}) \quad \text{S.43}$$

Here  $f_{lr}$  is the firing discharge rate of the slowly adapting lung stretch receptors (SARs).  $\tau_{lung}$  is the time constant of the receptor response to lung inflation.  $G_{al}$  is a constant gain factor and  $V_{lung}$  is the lung volume.

### **Integration of afferent input types in brainstem**

Afferent input types are combined in a linear manner prior to being received by the respective brainstem nuclei such as the nucleus ambiguus (NA) and dorsal motor nucleus of the vagus (DMV), included in the model.

As described in the “*NTS, NA, and the DMV Function and Role in Parasympathetic (Vagal) Outflow*” in the main text, the NA and DMV receive a linear combination of firing frequency signals generated by the NTS neuronal subtype:

$$f_{input,NA} = K_{br,NA}f_{br} + K_{cp,NA}f_{cp} + K_{lr,NA}f_{lr} \quad \text{S.44}$$

$$f_{input,DMV} = K_{br,DMV}f_{br} + K_{cp,DMV}f_{cp} + K_{lr,DMV}f_{lr} \quad \text{S.45}$$

$K_{xx,YY}$  represents a gain factor, or weight, of the firing frequency signal from the respective NTS neuronal subtype (br, cp, lr) to the respective brainstem nuclei (NA, DMV). Note that the  $K_{br,DMV}$  is set to 0 to remove any influence of baroreceptors have on the DMV. Concomitantly, a  $K_{lr,DMV}$  is set to 1 in order to facilitate an effect of lung tidal volume (mediated by lung stretch receptors in the NTS) on heart contractility, which is predominantly regulated by the DMV. This connection between the lung stretch receptors and DMV is thus an imposition placed in the model to maintain the overall relationship observed experimentally.<sup>10,11</sup>

## **Efferent sympathetic outflow**

Sympathetic efferent outflow is modeled to be dependent on the afferent input signals sent by the baroreceptor, cardiopulmonary, and lung stretch receptors. Moreover, the combined effects of these input signals affect sympathetic efferent outflow to different effector functions differently. Therefore, a series of calculations are included to determine *i)* the afferent firing frequency input that is then used to determine *ii)* the distinct sympathetic efferent outflow signals to the respective effector functions associated with the heart (*h*), peripheral circulation (*p*), and unstressed volumes (*v*)

$$f_{as,h} = G_{ab,h} * f_{br} - G_{alh} * f_{lr} + G_{ac,h} * f_{cp} \quad \text{S.46}$$

$$f_{as,p} = G_{ab,p} * f_{br} + G_{al,p} * f_{lr} + G_{ac,p} * f_{cp} \quad \text{S.47}$$

$$f_{as,v} = G_{ab,v} * f_{br} + G_{al,v} * f_{lr} + G_{ac,v} * f_{cp} \quad \text{S.48}$$

$G_{ab,j}$ , where *j* is a general index for the heart, peripheral circulation, or unstressed volume, represents a constant gain factor indicating how much influence each afferent input has on determining sympathetic efferent outflow. A factor of -1 is used for  $G_{al,h}$  as this provided the best fits for the model. The resulting  $f_{as,j}$  values are then used to determine sympathetic efferent outflow to the respective effector functions using a negative monotonic function to relate afferent activity to efferent neural pathways,

$$f_{es,h} = f_{es,\infty} + (f_{es,0} - f_{es,\infty}) * \exp(-k_{es} * f_{as,h}) \quad \text{S.49}$$

$$f_{es,p} = f_{es,\infty} + (f_{es,0} - f_{es,\infty}) * \exp(-k_{es} * f_{as,p}) \quad \text{S.50}$$

$$f_{es,v} = f_{es,\infty} + (f_{es,0} - f_{es,\infty}) * \exp(-k_{es} * f_{as,v}) \quad \text{S.51}$$

**Parasympathetic (vagal) efferent output** is described in detail in the main text.

### **Effector function regulation**

Physiological parameters affected by sympathetic and parasympathetic outflow include resistances, unstressed volumes, and cardiac elastances. Sympathetic outflow regulates resistances and unstressed volumes via a monotonic logarithmic static function, a low-pass first-order dynamics, and a time delay specific to each effector function.

$$\sigma_{\theta}(t) = \begin{cases} G_{\theta} * \ln[f_{es,j}(t - D_{\theta}) - f_{es,min} + 1], & f_{es,j} \geq f_{es,min} \\ 0 & , f_{es,j} < f_{es,min} \end{cases} \quad \text{S.52}$$

$$\frac{d\Delta\theta}{dt}(t) = \frac{1}{\tau_{\theta}} * (-\Delta\theta(t) + \sigma_{\theta}(t)) \quad \text{S.53}$$

$$\theta(t) = \Delta\theta(t) + \theta_0 \quad \text{S.54}$$

Where  $\theta$  represents generic controlled parameters (i.e. resistance or unstressed volume).  $\tau_\theta$  and  $D_\theta$  are the time constants and time delays associated with sympathetic regulatory mechanisms on these effector functions.  $G_\theta$  is a constant gain factor for the various effector functions and  $\theta_0$  represents constant values for respective effector functions. Note that  $f_{es,j}$  is used to represent the different sympathetic tones specific to a particular effector function.

### Ventricular Contractility

Because ventricular contractility is dependent on the balance of sympathetic and parasympathetic drive, similar to heart period, a similar approach is used to determine contractility. Thus, a linear interaction between sympathetic and parasympathetic effects on the inverse of  $E_{max,lv}$  is used

$$\sigma_{E,s}(t) = \begin{cases} -G_{s,E_{max}} * \ln[f_{es,h}(t - D_{E,s}) - f_{es,min} + 1], & f_{es,h} \geq f_{es,min} \\ 0 & , f_{es,h} < f_{es,min} \end{cases} \quad \text{S.55}$$

$$\frac{d\Delta\left(1/E_{max,lv}\right)_s(t)}{dt} = \frac{1}{\tau_{E,s}} * \left( -\Delta\left(1/E_{max,lv}\right)_s(t) + \sigma_{E,s}(t) \right) \quad \text{S.56}$$

$$\sigma_{E,v} = G_{E,v} * f_{ev,h}(t - D_{E,v}) \quad \text{S.57}$$

$$\frac{d\Delta\left(1/E_{max,lv}\right)_v(t)}{dt} = \frac{1}{\tau_{E,v}} * \left( -\Delta\left(1/E_{max,lv}\right)_v(t) + \sigma_{E,v}(t) \right) \quad \text{S.58}$$

$$\left(1/E'_{max,lv}\right) = \Delta\left(1/E_{max,lv}\right)_s + \Delta\left(1/E_{max,lv}\right)_v \quad \text{S.59}$$

$$E_{max,lv} = E'_{max,lv} + E_{max,lv,0} \quad \text{S.60}$$

Here,  $\tau_{E,s}$ , and  $\tau_{E,v}$ , represent the time constants associated with the sympathetic and parasympathetic regulatory mechanisms on contractility.  $D_{E,s}$  and  $D_{E,v}$  correspond to the time delays associated the sympathetic and parasympathetic mechanisms. Once  $1/E'_{max,lv}$  is determined,  $E_{max,lv}$  can easily be calculated using equation S.60.  $E_{max,lv,0}$  represents a constant, baseline elasticity value determined from experimental data collected from a dog whose stellate ganglion and vagal nerve fibers were denervated, effectively removing any autonomic influence.<sup>12</sup>

Equations similar to S.55-S.60 are used to determine  $1/E_{max,rv}$  (right ventricle). However, all gains were adjusted by a factor of (1/0.59), based on the ratio value used to relate contractility between the right and left ventricle used by Ursino originally.

### **Lung volume, thoracic, and abdominal pressures**

A linear relationship between lung volume and thoracic pressure is used to model lung volume measured by the lung stretch receptors:

$$V_{lung} = V_{lung,0} - 0.1 * P_{thor} \quad \text{S.61}$$

Thoracic pressure varies with time due to the effects of the respiratory cycle, which is modeled independently from any autonomic regulation. Parameters were chosen based on experimental work by <sup>13</sup>. Thoracic pressure varies linearly during respiration between a minimum of  $-9$  mmHg and a maximum of  $-4$  mmHg, which represents steady-state thoracic pressure during the respiratory pause, as modeled by the following equations:

$$P_{thor} = \begin{cases} P_{thor,max} - (P_{thor,max} - P_{thor,min}) * \frac{T_{resp}}{T_{insp}} * s & 0 \leq s \leq \frac{T_{insp}}{T_{resp}} * s \\ P_{thor,max} - \frac{(P_{thor,max} - P_{thor,min})}{T_{exp}} * (T_{insp} - T_{exp} - s * T_{resp}), & \frac{T_{insp}}{T_{resp}} \leq s \leq \frac{T_{insp}}{T_r} \\ P_{thor,max} & \frac{T_{insp} + T_{exp}}{T_{resp}} \leq s \leq 1 \end{cases} \quad \text{S.62}$$

Where  $T_{resp}$  is the period of respiration.  $T_{insp}$  is the inspiration time,  $T_{exp}$  is the expiration time.  $P_{thor,min}$  is the value of the intrathoracic pressure at the end of inspiration while  $P_{thor,max}$  is the max value of intrathoracic pressure at the end of expiration and throughout the respiratory pause, which takes place in between each respiration period. The parameter  $s$  is dimensionless, varying between 0 and 1, and represents the fraction of the respiratory cycle. A value of 0 represents the beginning of the respiration cycle. Similar to other parameters representing a fraction of cycle completion, an expression for  $s(t)$  has been



developed by Magosso et al. (2001) by introducing yet another state variable  $\varepsilon(t)$ , which is determined by the following equation<sup>14</sup>

$$\frac{d\varepsilon}{dt} = \frac{1}{T_{resp}} \quad \text{with } s(t) = \text{frac}(\varepsilon) \quad \text{S.63}$$

Abdominal pressure is modeled accordingly:

$$P_{abd} = \begin{cases} -2.5 * s * \frac{T_{resp}}{T_{insp/2}} - 4 & 0 < s < \frac{T_{insp/2}}{T_{resp}} \\ -2.5 & \frac{T_{insp/2}}{T_{resp}} < s < \frac{T_{insp}}{T_{resp}} \\ -2.5 * \frac{T_{insp} + T_{exp} - s * T_{resp}}{T_{exp}} & \frac{T_{insp}}{T_{resp}} < s < \frac{T_{insp} + T_{exp}}{T_{resp}} \\ -5 * \frac{T_{insp} + T_{exp} - s * T_{resp}}{T_{exp}} - 4 & \frac{T_{insp} + T_{exp}}{T_{resp}} < s < 1 \end{cases} \quad \text{S.64}$$

Where  $T_{resp}$  represents the respiratory period,  $T_{insp}$  represents the duration of inspiration and  $T_{exp}$  represents the duration of expiration.  $s$  is a dimensionless variable, similar to the variable  $u(t)$ , used to represent the fraction of the cardiac cycle that has completed. Here,  $s$  is calculated by solving for an additional state variable,  $\varepsilon$

$$\frac{d\varepsilon}{dt} = \frac{1}{T_{resp}} \quad \text{S.65}$$

$$s(t) = \text{frac}(\varepsilon) \quad \text{S.66}$$

Where the fractional portion  $\text{frac}(\varepsilon)$  resets the variable  $s(t)$  to zero once it reaches a value of 1.

## Model Parameters

We would like to emphasize that many of these parameter values are from source material and are provided here for the readers' convenience.<sup>1-4</sup> Interested readers are recommended to review this paper for a detailed description of the model. The model, created in the SIMULINK (R2020b) platform and associated MATLAB (R2020b) code are available on GitHub (<https://github.com/Daniel-Baugh-Institute/CardiovascularControl/tree/main/v03>; ver. 3, 2022).

Table S.1 Hemodynamic variables

<b>Model parameters</b>	<b>Corresponding physiological parameter</b>
$P_j$	Intravascular pressure
$V_{u,j}$	Unstressed volume
$F_j$	Blood flow
$C_j$	Compliance
$L_j$	Inertance
$R_j$	Resistances
$F_{o,r}$	Flow out of right ventricle
$F_{o,l}$	Flow out of left ventricle

Extended model parameter values for basal (healthy) state

Table S.2 Hemodynamic parameter values (vascular system)

Parameter	Value	Reference
Compliances (mL/mmHg)		
$C_{sa}$	0.28	2
$C_{sp}$	2.05	2
$C_{ep}$	1.36	5
$C_{mp}$	0.31	5
$C_{sv}$	43.11	5
$C_{ev}$	28.40	5
$C_{mv}$	6.60	5
$C_{tv}$	33	5
$C_{pa}$	0.76	2
$C_{pp}$	5.80	2
$C_{pv}$	25.37	2
Unstressed Volumes (mL)		
$V_{u,sa}$	0	2
$V_{u,sp}$	274.40	2
$V_{u,ep}$	274.1	5
$V_{u,mp}$	62.50	5
$V_{u,sv}^*$	1121	2
$V_{u,ev}^*$	1120	5
$V_{u,mv}^*$	255	5
$V_{u,tv}^*$	0	4
$V_{u,pa}^*$	0	2
$V_{u,pp}^*$	123	2
$V_{u,pv}^*$	120	2
Hydraulic Resistances (mmHg*s*mL <sup>-1</sup> )		
$R_{sa}$	0.06	2
$R_{sp}^*$	3.307	2
$R_{ep}^*$	1.725	5
$R_{mp}^*$	4.130	5
$R_{sv}$	0.038	2
$R_{ev}$	0.0197	5
$R_{mv}$	0.0848	5

$R_{tv}$	0.0054	5
$R_{pa}$	0.0230	2
$R_{pp}$	0.0894	2
$R_{pv}$	0.0056	2
Inertance (mmHg*ml*s <sup>-2</sup> )		
$L_{sa}$	2.2e-4	2
$L_{pa}$	1.8e-4	2

Table S.3 Hemodynamic parameters (left heart)

Parameter	Value	Units	Reference
$C_{la}$	19.23	mL/mmHg	2
$V_{u,la}$	25	mL	2
$R_{la}$	2.5e-3	mmHg*s*mL <sup>-1</sup>	2
$P_{0,lv}$	1.5	mmHg	2
$k_{E,lv}$	0.014	mL <sup>-1</sup>	2
$V_{u,lv}$	16.77	mL	2
$E_{max,lv,0}$	1.283	mmHg/mL	1
$k_{R,lv}$	3.75e-4	s/mL	2

Table S.4 Activation function parameters

Parameter	Value	Units	Reference
$k_{sys}$	0.075	sec <sup>2</sup>	2
$T_{sys,0}$	0.40	sec	2

Table S.5 Hemodynamic parameters (right heart)

Parameter	Value	Units	Reference
$C_{ra}$	31.25	mL/mmHg	2
$V_{u,ra}$	25	mL	2
$R_{ra}$	2.5e-3	mmHg*s*mL <sup>-1</sup>	2
$P_{0,rv}$	1.5	mmHg	2
$k_{E,rv}$	0.0110	mL <sup>-1</sup>	2
$V_{u,rv}$	40.8	mL	2
$E_{max,rv,0}$	0.7570	mmHg/mL	1
$k_{R,rv}$	1.4e-3	s/mL	2

Table S.6 Afferent input parameters (baroreceptors)

Parameter	Value	Units	Reference
$P_n$	92	mmHg	2
$f_{min}$	2.52	Hz	2
$f_{max}$	47.78	Hz	2
$k_a$	1.43**	mmHg	5
$\tau_z$	6.37	sec	2
$\tau_p$	2.076	Sec	2

Table S.7 Afferent input parameters (cardiopulmonary receptors)

Parameter	Value	Units	Reference
$P_{tn}$	10.80	mmHg	5
$f_{max,l}$	20	Hz	2
$k_l$	11.758	mmHg	5
$\tau_{cp}$	2	sec	5

Table S.8 Afferent input parameters (lung stretch receptors)

Parameter	Value	Units	Reference
$G_{al}$	23.291	v	5
$\tau_{lung}$	0.5	sec	5

Table S.9 Afferent firing frequency gains (to heart)

Parameter	Value	Units	Reference
$G_{ab,h}$	1	--	2
$G_{al,h}$	1.541	--	1 <sup>+</sup>
$G_{ac,h}$	2	--	5

<sup>+</sup> Note:  $G_{al,h}$  is multiplied by a gain factor of -1 in the Simulink model indicating the “inhibiting” effect lung stretch receptors have on the heart.

Table S.10 Afferent firing frequency gains (to peripheral circulation)

Parameter	Value	Units	Reference
$G_{ab,p}$	1	--	2
$G_{al,p}$	0.33	--	3
$G_{ac,p}$	2.5	--	5

Table S.11 Afferent firing frequency gains (to unstressed volumes)

Parameter	Value	Units	Reference
$G_{ab,v}$	1	--	2
$G_{al,v}$	0	--	5

$G_{ac,v}$	0	--	5
------------	---	----	---

Table S.12 Efferent sympathetic outflow parameters

Parameter	Value	Units	Reference
$f_{es,0}$	16.11	Hz	2
$f_{es,\infty}$	2.1	Hz	2
$f_{es,min}$	2.66	Hz	2
$k_{es}$	0.0675	Sec	2

Table S.13 Effector function regulation (gains)

Parameter	Value	Units	Reference
$G_{R,sp}$	0.695	mmHg*mL <sup>-1</sup> *v <sup>-1</sup>	2
$G_{R,ep}$	0.653	mmHg*mL <sup>-1</sup> *v <sup>-1</sup>	2
$G_{R,mp}$	2.81	mmHg*mL <sup>-1</sup> *v <sup>-1</sup>	5
$G_{Vu,sv}$	-265.4	mL/v	2
$G_{Vu,ev}$	-107.5	mL/v	5
$G_{Vu,mv}$	-25	mL/v	5
$G_{T,s}$	-0.13	v	2
$G_{T,v}$	0.09	v	2
$G_{S,Emax,lv}$	0.103	mmHg*mL <sup>-1</sup> *v <sup>-1</sup>	1
$G_{v,Emax,lv}$	0.205	mmHg*mL <sup>-1</sup> *v <sup>-1</sup>	1

Where v = spikes/s (i.e. Hz)

Table S.14 Effector function (time constants)

Parameter	Value	Units	Reference
$D_{R,sp}$	2	sec	2
$D_{R,ep}$	2	sec	2

$D_{R,mp}$	2	sec	5
$D_{V_u,sv}$	5	sec	2
$D_{V_u,sv}$	5	sec	5
$D_{V_u,mv}$	5	sec	5
$D_{T,s}$	2	sec	2
$D_{T,v}$	0.2	sec	2
$D_{E,s}$	2	sec	1
$D_{E,v}$	0.2	sec	1

Table S.15 Effector function (constants)

<b>Parameter</b>	<b>Value</b>	<b>Units</b>	<b>Reference</b>
$R_{sp,0}$	2.49	mmHg*s*mL <sup>-1</sup>	2
$R_{ep,0}$	0.78	mmHg*s*mL <sup>-1</sup>	2
$R_{mp,0}$	4.13	mmHg*s*mL <sup>-1</sup>	5
$V_{u,sv,0}$	1435.4	mL	2
$V_{u,ev,0}$	1247	mL	5
$V_{u,mv,0}$	290	mL	4
$T_0$	0.58	sec	2

Table S.16 Basal-Respiration

<b>Parameter</b>	<b>Value</b>	<b>Units</b>	<b>Reference</b>
$T_{insp}$	1.6	sec	4
$T_{resp}$	4.0	sec	4
$T_{exp}$	1.4	sec	4
$P_{thor,min}$	-9	mmHg	5
$P_{thor,max}$	-4	mmHg	5



## Parasympathetic (vagal) outflow

Table S.17 Neuronal subtype parameters (baroreceptor-input subtype)

Parameter	Value	Units	Reference
$f_{min,BR}$	0.30	Hz	1
$f_{max,BR}$	21.50	Hz	1
$f_{midpt,BR}$	37.07	Hz	1
$k_{BR}$	21.00	Hz	1

Table S.18 Neuronal subtype parameters (cardiopulmonary receptor-input subtype)

Parameter	Value	Units	Reference
$f_{min,CPR}$	0.45***	Hz	1
$f_{max,CPR}$	28.33***	Hz	1
$f_{midpt,CPR}$	10.20***	Hz	1
$k_{CPR}$	7.00	Hz	1

Table S.19 Neuronal subtype parameters (lung-stretch receptor input subtype)

Parameter	Value	Units	Reference
$f_{min,LSR}$	2.75	Hz	1
$f_{max,LSR}$	31.57	Hz	1
$f_{midpt,LSR}$	11.13	Hz	1
$k_{LSR}$	2.00	Hz	1

Table S.20 Nucleus ambiguus neuronal population parameters (heart rate)

<b>Parameter</b>	<b>Value</b>	<b>Units</b>	<b>Reference</b>
$f_{min,NA}$	4.88	Hz	1
$f_{max,NA}$	15.78	Hz	1
$f_{midpt,NA}$	59.83	Hz	1
$k_{NA}$	23.00	Hz	1

Table S.21 Nucleus ambiguus neuronal population parameters (contractility)

<b>Parameter</b>	<b>Value</b>	<b>Units</b>	<b>Reference</b>
$f_{min,NActr}$	0.61	Hz	1
$f_{max,NActr}$	11.00	Hz	1
$f_{midpt,NActr}$	12.81	Hz	1
$k_{NActr}$	7.00	Hz	1

Table S.22 Dorsal motor nucleus neuronal population (contractility)

<b>Parameter</b>	<b>Value</b>	<b>Units</b>	<b>Reference</b>
$f_{min,DMV}$	2.59	Hz	1
$f_{max,DMV}$	6.66	Hz	1
$f_{midpt,DMV}$	42.91	Hz	1
$k_{DMV}$	33.5	Hz	1

Table S.23 NTS subtype gains to NA and DMV

<b>Parameter</b>	<b>Value</b>	<b>Units</b>	<b>Reference</b>
$K_{BR,NA}$	1.0	--	1
$K_{CPR,NA}$	1.0	--	1
$K_{LSR,NA}$	1.0	--	1
$K_{BR,DMV}$	0.0	--	1
$K_{CPR,DMV}$	1.0	--	1
$K_{LSR,DMV}$	1.0	--	1

Table S.24 Respiratory sinus arrhythmia gating

<b>Parameter</b>	<b>Value</b>	<b>Units</b>	<b>Reference</b>
$K_{RSA}$	0.5	--	Estimated

Table S.25 RR interval elongation due to vagal firing

<b>Parameter</b>	<b>Value</b>	<b>Units</b>	<b>Reference</b>
$K_{RR,1}$	2.0	--	Estimated <sup>6</sup>
$K_{RR,2}$	1.9	--	Estimated <sup>6</sup>
$\tau_{RR,1}$	0.01	--	Estimated <sup>6</sup>
$\tau_{RR,2}$	0.07	--	Estimated <sup>6</sup>
$\tau_{RR,3}$	0.3	--	Estimated <sup>6</sup>

$\tau_{RR,4}$	0.3	--	Estimated <sup>6</sup>
$\xi_{RR}$	0.6	--	Estimated <sup>6</sup>

Table S.26 Principal neurons that receive nucleus ambiguus inputs neuronal population

<b>Parameter</b>	<b>Value</b>	<b>Units</b>	<b>Reference</b>
$f_{min,PN_{NA}}$	0.86	Hz	Estimated
$f_{max,PN_{NA}}$	12.62	Hz	Estimated
$f_{midpt,PN_{NA}}$	13.81	Hz	Estimated
$k_{PN_{NA}}$	3.23	Hz	Estimated

Table S.27 Principal neurons that receive dorsal motor nucleus inputs neuronal population

<b>Parameter</b>	<b>Value</b>	<b>Units</b>	<b>Reference</b>
$f_{min,PN_{DMV}}$	2.42	Hz	Estimated
$f_{max,PN_{DMV}}$	17.72	Hz	Estimated
$f_{midpt,PN_{DMV}}$	14.18	Hz	Estimated
$k_{PN_{DMV}}$	13.36	Hz	Estimated
$\tau_{PN_{DMV}}$	0.3	s	Estimated <sup>15</sup>

Table S.28 Local circuit neurons

<b>Parameter</b>	<b>Value</b>	<b>Units</b>	<b>Reference</b>
$f_{min,LCN}$	1.99	Hz	Estimated
$f_{max,LCN}$	18.38	Hz	Estimated
$f_{midpt,LCN}$	521.22	Hz	Estimated
$k_{LCN}$	3.00	Hz	Estimated
$K_{LCN_{BR}}$	2.66	--	Estimated
$K_{LCN_{CP}}$	5.64	--	Estimated
$K_{LCN_{fesh}}$	0.07	--	Estimated
$K_{LCN_{fev}}$	3.33	--	Estimated

\* These parameter values can also be calculated from the model equations.

\*\* This parameter value was corrected from Park et al. (2020) after cross-checking with Table 1 and Equation (A7) in Magosso et al. (2002).<sup>1,5</sup>

\*\*\* Alternate parameter values used in Park et al. (2020).<sup>1</sup> As explained in the main text, the model is highly non-linear and the available experimental data are measurements of overall cardiac function and electrophysiological behavior in response to a stimulus. Thus, the use of multiple sigmoidal functions to represent the dynamic behavior of neuronal subpopulations raises the possibility of over-parametrization. Therefore, several distinct sets of parameter values could produce similar predicted cardiovascular system behaviors. In fact, previous experiments analyzing transcriptomic profiles of single neurons in the brainstem and ICN have shown that neurons exist in

multiple functional states that may be described by these distinct sets of parameter values.<sup>16,17</sup> Thus, these parameter values are an alternative set of parameter values identified in Park et al. (2020) that describe a plausible functional state of the neuronal group.<sup>1</sup>

## **Self-assessment of conformance to the Ten Simple Rules of Credible Practice in Modeling and Simulation in Healthcare**

Closed-loop modeling of intrinsic cardiac nervous system contributions to respiratory sinus arrhythmia

The following self-assessment is based on the rules specified in Erdemir et al. (2020).<sup>18</sup> A rubric is available at: <https://www.imagwiki.nibib.nih.gov/content/10-simple-rules-conformance-rubric>

Date of initial self-assessment: October 06, 2022

Date of revised self-assessment: December 9, 2022

**Rule 1: Define context clearly:** Develop and document the subject, purpose, and intended use(s) of the model or simulation.

**Current Conformance Level:** Comprehensive

**Model Context:** Model of neural control of cardiovascular behavior and its interaction with respiratory behavior

**Primary goal of the model/tool/database:** The primary objective of the modeling study was to evaluate the role of neural signals in controlling the dynamic behavior of the heart, particularly in regulating cardiovascular metrics such as heart rate and blood pressure. We also seek to understand neural control of respiratory sinus arrhythmia, a natural acceleration and deceleration of heart rate in synchronization with respiration, which is characteristic of good cardiovascular health.

Our model builds on a previously developed model of neural control of the heart.<sup>1</sup> We extended this model by integrating the “little brain of the heart”, the intrinsic cardiac nervous system (ICN), to study its contributions to cardiovascular control. This newly developed model with the ICN also integrates modeling of the cardiac phase-dependent effect of parasympathetic activity on heart rate deceleration and gating of signals in the brainstem in based on respiratory phase to represent a possible mechanism of respiratory sinus arrhythmia (RSA). Our expanded model can be utilized to explore the role of the ICN on beat-to-beat cardiovascular behavior, specifically RSA. Simulations can be performed to explore regulation of



cardiovascular behavior in response to changes in lung tidal volume and electrical stimulation of the vagus nerve, which connects the brain and the heart.

**Biological Domain of the Model:** Cardiovascular system and autonomic control

**Structures of the Model:** Heart, vasculature, brainstem, intrinsic cardiac nervous system

**Spatial Scales Included in the Model:**  $10^{-2}$  to  $10^{-1}$  meters

**Time Scales Included in the Model:** 0 to 200 seconds

**Other uses for the model (optional):**

**Additional comments about the model's context (optional):** While the cardiovascular metrics used to validate the model are from humans, data from dogs and pigs was used to select the parameters for some neural control portions of the model. This information should be considered when using the model for clinical applications.

**Revision summary:**

This section did not change during revision.

**Rule 2: Use contextually appropriate data:** Employ relevant and traceable information in the development or operation of a model or simulation.

**Current Conformance Level:** Extensive

<b>Data for building the model</b>	<b>Published ?</b>	<b>Private ?</b>	<b>How is credibility checked?</b>	<b>Current Conformance Level</b>
in vitro (primary cells cell, lines, etc.)	Yes	No	The source data is confirmed to meet detailed data requirements for consistency and source description	Adequate
ex vivo (excised tissues)	N/A	N/A	N/A	N/A
in vivo pre-clinical (lower-level organism or small animal)	N/A	N/A	N/A	N/A
in vivo pre-clinical	Yes	No	The source data is	Adequate

(large animal)			confirmed to meet detailed data requirements for consistency and source description	
Human subjects/clinical	Yes	No	the source data is confirmed to meet detailed data requirements for consistency and source description	Extensive

**Revision summary:**

This section did not change during revision.

<b>Data for validating the model</b>	<b>Published ?</b>	<b>Private ?</b>	<b>How is credibility checked?</b>	<b>Current Conformance Level</b>
in vitro (primary cells cell, lines, etc.)	N/A	N/A	N/A	N/A
ex vivo (excised tissues)	N/A	N/A	N/A	N/A
in vivo pre-clinical (lower-level organism or small animal)	N/A	N/A	N/A	N/A
in vivo pre-clinical (large animal)	Yes	No	The source data is confirmed to meet detailed data requirements for consistency and source description	Extensive
Human subjects/clinical	Yes	No	The source data is confirmed to meet detailed data requirements for	Extensive

			consistency and source description	
--	--	--	---------------------------------------	--

**Revision summary:**

This section did not change during revision.

**Rule 3: Evaluate within context:** Perform verification, validation, uncertainty quantification, and sensitivity analysis of the model or simulation with respect to the reality of interest and intended use(s) of the model or simulation.

**Current Conformance Level:** Extensive

	<b>Who Does It?</b>	<b>When does it happen?</b>	<b>How is it done?</b>	<b>Current Conformance Level</b>
<b>Verification</b>	Developer	During development	Comparison of model output with published animal and human data	Extensive
<b>Validation</b>	Lab Member	During development	Model was used to reproduce simulations and figures	Extensive
<b>Uncertainty Quantification</b>	User performs uncertainty quantification	Can be performed after every	User discretion	Adequate

		new simulation		
<b>Sensitivity Analysis</b>	Developer	Can be performed after every new simulation	PAWN sensitivity analysis files are provided in the supplementary material <sup>19</sup>	Adequate

**Revision summary:**

A global sensitivity analysis using the PAWN method was added in Supplementary Figure 1. Files for running the analysis were added to the model GitHub repository.

**Rule 4: List limitations explicitly:** Provide restrictions, constraints, or qualifications for or on the use of the model or simulation for consideration by the users or customers of a model or simulation.

**Current Conformance Level:** Comprehensive

<b>Disclaimer statement (explain key limitations)</b>	<b>Who needs to know about this disclaimer?</b>	<b>How is this disclaimer shared with that audience?</b>	<b>Current Conformance Level</b>
Limited animal electrophysiology data for parameterization	Users	Stated explicitly in the main text	Comprehensive
Model tuning and validation data is from animals that were under anesthesia when the data was collected. Anesthesia is	Users	Stated explicitly in the main text	Comprehensive



known to affect heart rate and blood pressure.			
Static rather than dynamic firing rate model used to represent ICN neuronal population activity	Users	Stated explicitly in the main text	Comprehensive

**Revision summary:**

Use of static firing rate model to represent ICN neurons added as a limitation.

**Rule 5: Use version control:** Implement a system to trace the time history of modeling and simulation activities including delineation of each contributors' efforts.

**Current Conformance Level:** Extensive

	<b>Naming Conventions?</b>	<b>Repository?</b>	<b>Code Review?</b>
<b>individual modeler</b>	Yes	GitHub	Yes
<b>within the lab</b>	Yes	GitHub	Yes
<b>collaborators</b>	N/A	N/A	N/A

**Revision summary:**

This section did not change during revision.

**Rule 6: Document appropriately:** Maintain up-to-date informative records of all modeling and simulation activities, including simulation code, model mark-up, scope and intended use of modeling and simulation activities, as well as users' and developers' guides.

**Current Conformance Level:** Extensive

	<b>Current Conformance Level</b>
<b>Code Commented?</b>	Extensive: comments made in the model file
<b>Scope and intended use described?</b>	Extensive: described in the main text
<b>User's Guide</b>	Extensive: described in the main text and supplemental files
<b>Developer's Guide?</b>	Partial: Details of model development in methods of main text

**Revision summary:**

This section did not change during revision.

**Rule 7: Disseminate broadly:** Share all components of modeling and simulation activities, including simulation software, models, simulation scenarios and results.

**Current Conformance Level:** Extensive

<b>Target Audience(s):</b>	<b>“Inner Circle”</b>	<b>Scientific Community</b>	<b>Public</b>
<b>Simulations</b>			Description of simulations stated in the main text.
<b>Models</b>			Model files present on GitHub.
<b>Software</b>		Some simulations were run in parallel using the University of Delaware’s DARWIN computing resources. Any available high performance computing cluster	MATLAB and Simulink were used, both of which are publicly available for a fee. All figures can be generated using solely MATLAB and Simulink.

		should be able to run the simulations.	
<b>Results</b>			Described in main text.
<b>Implication of Results</b>			Described in main text.

**Revision summary:**

This section did not change during revision.

**Rule 8: Get independent reviews:** Have the modeling and simulation activity reviewed by nonpartisan third-party users and developers.

**Current Conformance Level:** Extensive

<b>Reviewer(s) name and affiliation</b>	<b>Varghese Kurian (University of Delaware)</b>
When was the review performed	October 7, 2022
How was review performed and outcomes of the review?	A member of the research group, not involved in the present study performed the review.  Model files and tables in the text were cross-checked for consistency.  Simulation results and figures were independently reproduced using the files provided on GitHub.

**Revision summary:**

Model files involving the PAWN sensitivity analysis were cross-checked for consistency and figures were independently reproduced using the files provided on GitHub. The other model files were not changed and so the initial independent review was deemed adequate.

**Rule 9: Test competing implementations:** Use contrasting modeling and simulation implementation strategies to check the conclusions of different strategies against each other.

**Current Conformance Level:** Adequate

	<b>Yes or No (briefly summarize)</b>
<b>Were competing implementations tested?</b>	<p>Yes, in multiple stages.</p> <p>Competing implementations were tested and compared by the first author of the paper during the initial manuscript preparation.</p>
<b>Did this lead to model refinement or improvement?</b>	<p>Yes, the model was refined and improved whenever inconsistencies with experimental data on cardiovascular metrics such as heart rate, left ventricular elastance, and blood pressure arose. Specifically, parameters describing ICN neuronal groups were re-tuned and vagal nerve stimulation modeling was refined.</p>

**Revision summary:**

This section did not change during revision.



**Rule 10: Conform to standards:** Adopt and promote generally applicable and discipline specific operating procedures, guidelines, and regulations accepted as best practices.

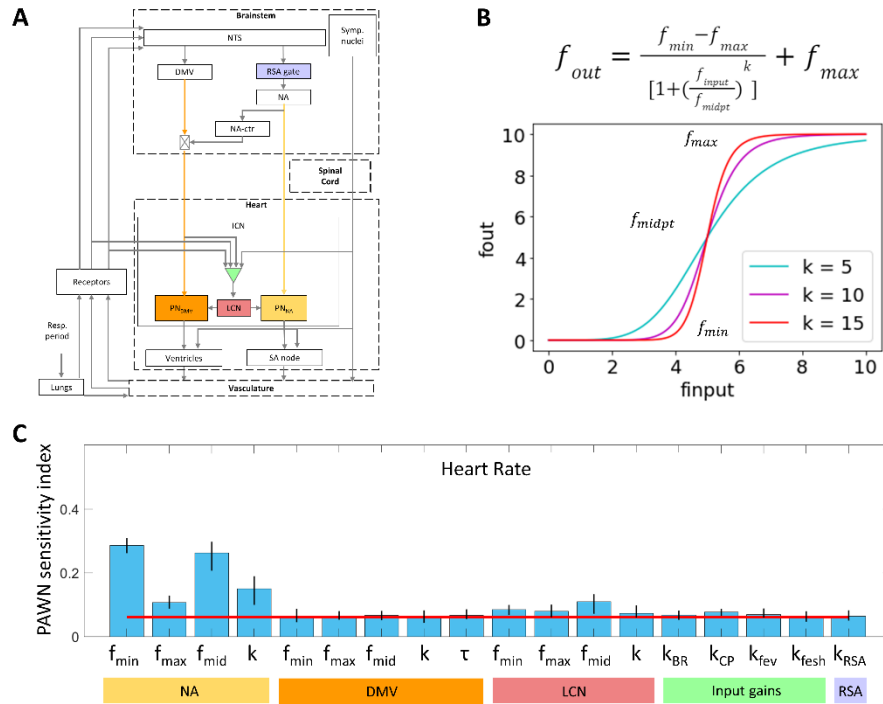
**Current Conformance Level:** Adequate

	<b>Yes or No (briefly summarize)</b>
<b>Are there operating procedures, guidelines, or standards for this type of multiscale modeling?</b>	Yes, as described in the credible practice of modeling and simulation in healthcare: ten rules from a multidisciplinary perspective. <sup>18</sup>
<b>How do your modeling efforts conform?</b>	Our model is implemented in the widely used MATLAB and Simulink platforms for computational modeling. The code is commented at critical locations to aid the reader.

**Revision summary:**

This section did not change during revision.

## Sensitivity Analysis



**Supplementary Figure S.1.** PAWN global sensitivity analysis of parameters affecting heart rate.<sup>19</sup> Heart rate was measured as the average over a 15 s period.<sup>20</sup> Sensitivity indices range between 0 and 1, with 0 indicating that the model parameter has no impact on heart rate, and 1 indicating that the parameter of interest has a major influence on heart rate. Parameters with a sensitivity index above the red line are significant. Parameters were varied over a  $\pm 3$  fold range from the nominal value and six conditioning intervals were used. Each error bar represents the 95% confidence interval of the sensitivity index based on bootstrapping tests that involved 3000 iterations of a random sampling

of simulated HR. The role of model parameters are shown in (A) and correspond to the parameters in (B).  $f_{\min}$ , minimum output firing frequency for a neural population;  $f_{\max}$ , maximum output firing frequency for a neural population;  $f_{\text{mid}}$ , midpoint firing frequency for a neural population;  $k$ , gain describing the responsiveness of a neural population to a change in input firing frequency;  $k_{\text{BR}}$ , gain of baroreceptor input to LCNs;  $k_{\text{CP}}$ , gain of cardiopulmonary receptor input to LCNs;  $k_{\text{fev}}$ , gain of combined DMV and NA-ctr input to LCNs;  $k_{\text{resh}}$ , gain of sympathetic input to LCNs;  $k_{\text{RSA}}$ , gain of RSA gate.

To understand the relative contribution of each ICN neuronal parameter to overall cardiovascular behavior and prioritize parameters for further investigation, we performed a global sensitivity analysis. A density-based sensitivity analysis known as PAWN was used to determine relative sensitivity for heart rate.<sup>19</sup> A density-based approach was selected because the underlying distribution of the outputs was unknown. To determine the underlying distribution, PAWN uses cumulative density functions (CDF) to characterize the model output of interest and determine the output sensitivity to the input parameter input of interest. Two sets of simulations are performed. The first set varies all parameter inputs simultaneously to produce unconditional CDFs. The second set varies all inputs except the parameter of interest to produce conditional CDFs. To determine the sensitivity of the output parameter to changes in the input parameter of interest, the distance between the unconditional and conditional CDFs is quantified using the

Komogorov-Smirnoff (KS) statistic. If the conditional and unconditional CDFs are close together then the output is sensitive to that parameter because varying other parameters did not cause a significant change in the output. If they are far apart then the output is not sensitive to the input parameter of interest. Because the KS statistic is dependent upon the value of the constant parameter, the PAWN method determines the KS statistic across multiple values. To combine these statistics, we use a summary statistic (e.g. median) to characterize the distribution of the KS statistic. This summary statistic varies from 0 to 1 with a larger value indicating a greater parametric influence on the output. To determine a threshold value for significant summary statistics, the PAWN method introduces a dummy parameter, which is known to have no effect on the output. If the summary statistic of a parameter is above this value, it is likely the output is sensitive to that input parameter. In this analysis, we performed 3000 simulations and checked for convergence. by performing additional simulations and confirming that the results did not change. The PAWN method also includes bootstrapping to determine 95 percent confidence intervals for each sensitivity index.

**Calculation of cardiovascular metric changes from Yamakawa et al. 2014**

	Baseline		Stimulation		% change
	Mean	SE	Mean	SE	
HR (bpm)	84	4	73	5	13
SBP (mm Hg)	119	8	111	8	7
DBP (mm Hg)	83	9	74	9	11

**Table S.29.** Analysis of percent change in heart rate from baseline to stimulation.<sup>21</sup>

Values shown are for left vagus nerve stimulation. HR, heart rate; SBP, systolic blood pressure; DBP, diastolic blood pressure.

## Supplemental File References

1. Park JH, Gorky J, Ogunnaike B, Vadigepalli R, Schwaber JS. Investigating the Effects of Brainstem Neuronal Adaptation on Cardiovascular Homeostasis. *Front Neurosci.* 2020;14:470.
2. Ursino M. Interaction between carotid baroregulation and the pulsating heart: a mathematical model. *Am J Physiol.* 1998;275(5):H1733-47.
3. Ursino M, Magosso E. Acute cardiovascular response to isocapnic hypoxia. I. A mathematical model. *Am J Physiol Heart Circ Physiol.* 2000;279(1):H149-65.
4. Magosso E, Ursino M. Cardiovascular response to dynamic aerobic exercise: A mathematical model. *Med Biol Eng Comput.* 2002;40(6):660-674.
5. Magosso E, Cavalcanti S, Ursino M. Theoretical analysis of rest and exercise hemodynamics in patients with total cavopulmonary connection. *American Journal of Physiology-Heart and Circulatory Physiology.* 2002;282(3):H1018-H1034. doi:10.1152/ajpheart.00231.2001
6. Iano TL, Levy MN, Lee MH. An acceleratory component of the parasympathetic control of heart rate. *Am J Physiol.* 1973;224(5):997-1005.
7. Levy MN, Iano T, Zieske H. Effects of repetitive bursts of vagal activity on heart rate. *Circ Res.* 1972;30(2):186-195.

8. Scholkopf B, Peters J, Janzing D. *Elements of Causal Inference: Foundations and Learning Algorithms*. MIT Press; 2017.
9. Sundaramoorthy AS, Varanasi SK, Huang B, Ma Y, Zhang H, Wang D. Sparse Inverse Covariance Estimation for Causal Inference in Process Data Analytics. *IEEE Trans Control Syst Technol*. 2022;30(3):1268-1280.
10. Greenwood PV, Hainsworth R, Karim F, Morrison GW, Sofola OA. Reflex inotropic responses of the heart from lung inflation in anaesthetized dogs. *Pflugers Arch*. 1980;386(2):199-205.
11. Hainsworth R. Circulatory responses from lung inflation in anesthetized dogs. *Am J Physiol*. 1974;226(2):247-255.
12. Suga H, Sagawa K, Kostiuik DP. Controls of ventricular contractility assessed by pressure-volume ratio, Emax. *Cardiovasc Res*. 1976;10(5):582-592.
13. Moreno AH, Katz AI, Gold LD. An integrated approach to the study of the venous system with steps toward a detailed model of the dynamics of venous return to the right heart. *IEEE Trans Biomed Eng*. 1969;16(4):308-324.
14. Magosso E, Ursino M. A mathematical model of CO<sub>2</sub> effect on cardiovascular regulation. *Am J Physiol Heart Circ Physiol*. 2001;281(5):H2036-52.

15. Falkenburger BH, Jensen JB, Hille B. Kinetics of M1 muscarinic receptor and G protein signaling to phospholipase C in living cells. *J Gen Physiol.* 2010;135(2):81-97.
16. Park J, Brureau A, Kernan K, et al. Inputs drive cell phenotype variability. *Genome Res.* 2014;24(6):930-941.
17. Moss A, Robbins S, Achanta S, et al. A single cell transcriptomics map of paracrine networks in the intrinsic cardiac nervous system. *iScience.* 2021;24(7):102713.
18. Erdemir A, Mulugeta L, Ku JP, et al. Credible practice of modeling and simulation in healthcare: ten rules from a multidisciplinary perspective. *J Transl Med.* 2020;18(1):369.
19. Pianosi F, Wagener T. Distribution-based sensitivity analysis from a generic input-output sample. *Environmental Modelling & Software.* 2018;108:197-207.
20. Kobayashi M, Massiello A, Karimov JH, Van Wagoner DR, Fukamachi K. Cardiac autonomic nerve stimulation in the treatment of heart failure. *Ann Thorac Surg.* 2013;96(1):339-345.
21. Yamakawa K, So EL, Rajendran PS, et al. Electrophysiological effects of right and left vagal nerve stimulation on the ventricular myocardium. *Am J Physiol Heart Circ Physiol.* 2014;307(5):H722-31.